# Waveform Tomography of a 2-D Full Wavefield, Elastic, Wide Angle, Synthetic Dataset.

*A. Brenders and R. Gerhard Pratt, Queen's University, Kingston, Ontario, Canada.*

## Abstract

Using a starting model obtained from travel time inversion and an extremely low starting frequency, acoustic, frequency-domain waveform inversion methods are applied to synthetic time domain data. The synthetic data were generated in a blind test, using an elastic finite difference method in a deep crustal model. A waveform inversion strategy was developed that relies on preconditioning and iterative up-scaling of the input data and the inversion result. The solution obtained predicts the input data to a high degree of accuracy for each chosen data frequency. Comparison of the original, time domain data (bandpass filtered) and results from time domain forward modelling through the final inversion model model reveals a satisfying match.

## Introduction

In waveform tomography, the goal is to recover a model by iteratively minimizing the misfit between the observed data and the data calculated from forward modelling in a "best fit" model. Due to the high computational cost of calculating the synthetic data, the inverse problem is solved by local methods (Tarantola, 1984). Previous work has shown that the waveform inverse problem possesses a high degree of non-linearity, which can cause a solution of the misfit function to converge to a local rather than a global minimum (Sirgue, 2003). The success of waveform tomography is typically dependent upon the starting model accuracy and the minimum inversion frequency.

By preconditioning the update images and the data residuals with a variety of techniques, the convergence of the waveform tomography can be improved. In the absence of any direct knowledge of the subsurface (as in the blind test described herein), the efficacy of the waveform tomography approach can only be evaluated by a comparison of the original data with the data predicted in the best-fit model.

## 2-D Visco-elastic crustal model

A synthetic wide-angle dataset was obtained from the CCSS workshop organizers (courtesy of Colin Zelt and John Hole). The data were computed in a realistic, 2-D crustal model approximately 250 km wide and 45 km deep. Vertical and horizontal component data for 51 shots were calculated using a 2-D visco-elastic code. Vertical and horizontal displacements were recorded for each shot at a total of 2779 receiver locations.

## Data preparation

Our waveform tomography method uses an acoustic wave equation method. It was decided to use only the vertical component of the elastic data in this inversion study. Prior to inversion, the waveform data were bandpass filtered to remove all frequencies above 2 Hz, and spatially sub-sampled by selecting only every 10th receiver. A coarser grid spacing allows the inversion to proceed more rapidly, and mitigates the inherent nonlinearities in the waveform data which are less severe at the lower (somewhat unrealistic) frequencies. As the inversion progressed, more data (every 5th receiver, and then every 2nd receiver) and higher frequencies (up to nearly 7 Hz) were included to improve the spatial resolution. Since the

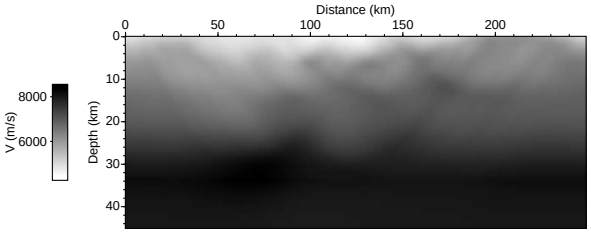


Fig. 1: First arrival travel time inversion result (courtesy of Colin Zelt). This was the starting model used in the inversion.

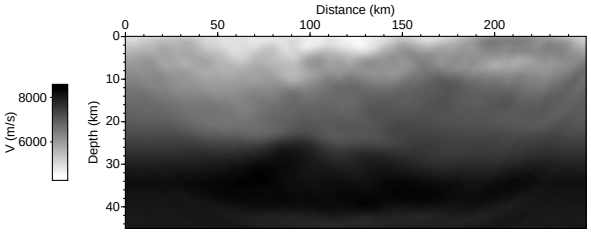


Fig. 2: Waveform tomography result after inverting from 0.8 to 2.0 Hz starting from the travel time inversion model, inverting a 3 s window of data, sub-sampled every 10th receiver, and using a time damping factor of $\tau$ =10 s.

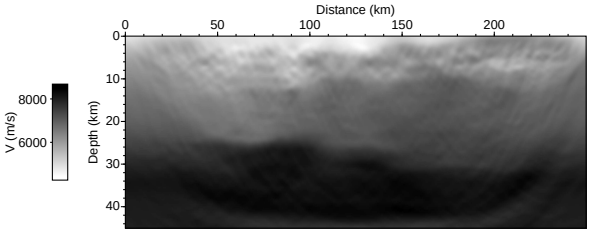


Fig. 3: Waveform tomography result after inverting from 0.8 to 4.0 Hz, starting from model shown in Figure 2. In this case a larger, 6 s window of data was used, a larger number of receivers was used (every 5th), and a larger time damping factor of $\tau$ = 20s was used.

near offset waveforms are dominated by ground roll, it was also desirable to preclude these data from the inversion. This was done by the application of an offset-dependent cosine taper in the frequency domain data in order to remove the nearest offsets from the inversion procedure.

To add stability to the inversion and to remove the obvious direct shear wave events, the data were time-windowed to include only waveforms occurring within a 3 s window starting at the picked first arrival times. This data window was subsequently increased to 6 s. The data were also preconditioned by applying a "time-domain damping factor" during the inversion procedure, which exponentially damps the input data as a factor of time. Initially a decay factor of $\tau = 10\,s$ was used; this was subsequently reduced to a factor of $\tau = 20\,s$ in order to try to give later arrivals more weight in the inversion.

Following bandpass filtering, spatial subsampling, time windowing and time domain damping, the data were transformed into the frequency domain in preparation for frequency domain waveform tomography (after Pratt 1999). In order to fit a time series 5 s long, a frequency sample interval of 1 / 5 s = 0.2 Hz is required. We chose to use this sample interval throughout the inversion, since we were primarily concerned with fitting the initial few seconds of each waveform.

The starting model for waveform tomography was obtained in a separate study (courtesy of Colin Zelt), by hand picking all arrival times on the synthetic data, and applying a travel time tomography method (Zelt and Barton, 1998). The result is shown in Figure 1. This model was re-sampled onto a grid appropriate for low frequency modelling; a grid spacing of $\Delta$ =1 km will contain at least 4 grid points per wavelength at 1 Hz. This level of spatial sampling of the waveform is considered sufficiently accurate for frequency domain finite differences (Jo

et al., 1996). At the later stages of the inversion this was eventually reduced to $\Delta$ =0.16 km.

Inspection of the original vertical component time domain data and our initial acoustic synthetic time domain data (as modelled through the starting model), indicate a dramatic disparity in the amplitude values and their decay with offset. This disparity is largely due to the difference in radiation pattern for an elastic wave point force used in the original data, as compared with the acoustic wave explosion source used in our approach. The disparity in the inelastic attenuation factors also plays a role (we used an infinite Q model). In order to be able to invert data from all offset ranges we found it essential to manipulate the input data to match the amplitude decay of the synthetic model data.

## Waveform Inversion

To optimize the convergence of the waveform tomography, a multi-scale approach was taken in designing the inversion scheme: We started our inversions using low frequencies, a coarse grid spacing, and coarse data sampling, allowing initial results to be obtained rapidly. The first inversion pass was performed using data frequencies from 0.8 Hz to 2 Hz, with the original travel time inversion model as the starting model. The resulting model was then interpolated onto a finer grid, and inversion was performed from 0.8 Hz to 4 Hz. In a final pass, this model was interpolated onto a finer grid still, allowing an inversion of frequencies from 2 Hz to 6.25 Hz.

As a part of our multi-scale approach, initial inversions with the lowest frequency data were subjected to a 2-D, low-pass wavenumber filter. The intended effect is that the unstable, high wavenumber components in the model are suppressed, and the low wavenumber components are boosted to enhance convergence. We adjusted the wavenumber filter to suppress lateral variations preferentially over vertical variations. As the inversion proceeded to higher frequencies the wavenumber filter was relaxed, allowing larger wavenumbers to contribute and improving the spatial resolution of the results.

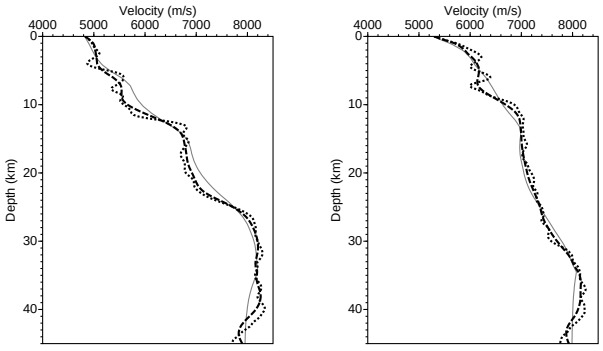


Fig. 4: Velocity traces at 90 km and 182 km along the model. Lines show the starting model (gray), the model from the 0.8 to 2 Hz inversion (dashed), and the model from the 0.8 to 4 Hz inversion (dotted).

A source signature was extracted directly from the data, using the method described in Pratt (1999). This was performed before each step in the waveform tomography. As the inversion scheme was scaled upward, the bandwidth of the data was increased, and a more realistic looking source was obtained.

Inversion results are presented in Figures 2 and 3. A gradual introduction of high resolution features can be observed as the inversion proceeds. A set of velocity profiles from approximately 90 km (Figure 4) and 182 km (Figure 4) along the model show the starting model (in light gray), the intermediate inversion model (dashed) and the final inversion model (dotted). These 1-D velocity profiles indicate the inversion is adding structure and complexity to the starting model with each subsequent pass.

In order to evaluate the efficacy of the waveform tomography results, a 10 s length of the original, unfiltered data is shown for a single shot point, located at 109.98 km (Figure 5 (a)). A sub-sample of this real dataset (every 5th receiver) is shown for the same shot, after low

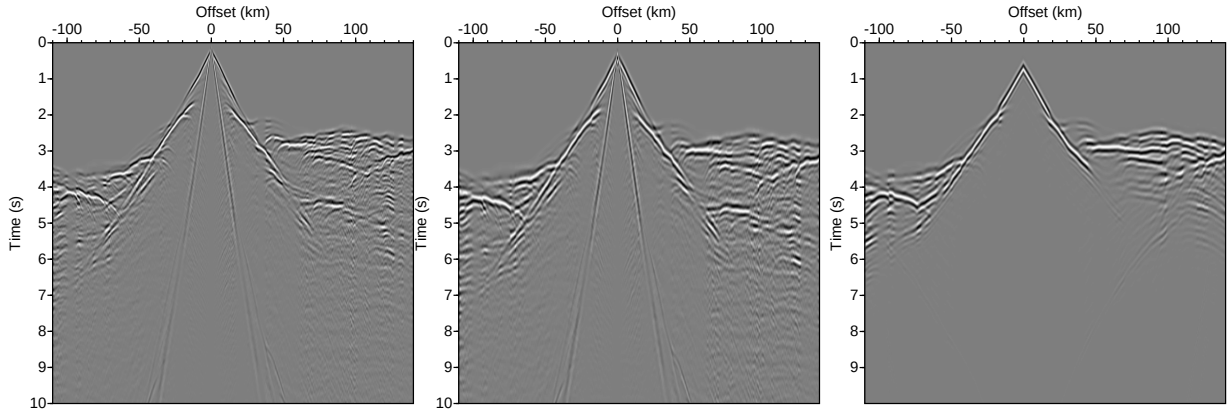


(a) Normalized time domain data for shot 23.

(b) 8 Hz Bandpass Filtered Data, Sub-Sampled Every 5th Receiver

(c) Forward modeled data, over 320 frequencies, on a grid with a spacing 0.16 km.

Fig. 5: Normalized time domain data for shot 23.

pass filtering to 8 Hz (Figure 5 (b)). The time domain forward modelling result, using 320 frequencies, is presented for comparison (Figure 5 (c)). The recovery of a waveform that matches the original data in many respects is encouraging, considering the limited number of data frequencies (80) that were used in the inversion.

## Conclusions and Future Work

Work is currently underway to complete waveform tomography with higher frequencies than 4 Hz. Computational limitations suggest the maximum invertible frequency may be as high as 8 Hz. A decrease in the frequency step size between simultaneous inversion frequencies (corresponding to the increased data window of 6 s used in the inversion) could also be performed to further the results.

### Acknowledgments

We gratefully thank Colin Zelt for providing the starting velocity model and the first arrival times used in this work, and John Hole and Colin Zelt for providing the data in the first place.

## References

Jo, C.-H., Shin, C., and Suh, J. H., 1996, An optimal 9-point, finite-difference, frequency-space, 2-d scalar wave extrapolator: Geophysics, **61**, no. 02, 529–537.

Pratt, R. G., 1999, Seismic waveform inversion in the frequency domain, part 1: Theory and verification in a physical scale model: Geophysics, **64**, no. 3, 888–901.

Sirgue, L., 2003, Inversion de la forme d'onde dans le domaine frequentiel de donnees sismiques grands offsets: Ph.D. thesis, Ecole Normale Superieure de Paris.

Tarantola, A., 1984, Inversion of seismic reflection data in the acoustic approximation: Geophysics, **49**, no. 08, 1259–1266.

Zelt, C. A., and Barton, P. J., 1998, 3D seismic refraction tomography: A comparison of two methods applied to data from the faeroe basin: J. Geophys. Res., **103**, 7187–7210.